sustainability

MDPI

Article

Numerical and Experimental Investigation of the Seismic Effect of a Two-Stage Seismic Isolation Method

Tianbo Peng [1,2], Jianyu Guan [2] and Yicheng Wu [2,*]

[1] State Key Laboratory of Disaster Reduction in Civil Engineering, Tongji University, Shanghai 200092, China
[2] College of Civil Engineering, Tongji University, Shanghai 200092, China
* Correspondence: 1630414@tongji.edu.cn

Abstract: In order to improve the post-earthquake resilience of bridge structures, a Two-Stage seismic isolation method is proposed in this paper. According to the method, the restoring force and horizontal stiffness are smaller in the first stage and become much larger in the second stage. Therefore, a new kind of seismic isolation device, Two-Stage Friction Pendulum Bearing (TSFPB for short), is invented based on the traditional friction pendulum bearing (FPB for short). In this paper, the geometry configuration, sliding states and hysteresis characteristics of the bearing are first introduced with a theoretical approach. Then the hysteresis curve of the TSFPB is verified experimentally and the simulation method of the bearing in an FEM software is proposed. Last, a numerical analysis for an actual highway girder bridge is carried out to compare the seismic design method recommended in this paper with the conventional seismic isolation method. It is found that the Two-Stage seismic isolation method has an adaptive restoring force, horizontal stiffness and energy dissipation mechanism for different seismic intensity levels and better seismic performance compared with a conventional seismic isolation method. In addition, bridges with TSFPBs have smaller residual displacements and better post-earthquake resilience than those with traditional FPBs.

Keywords: Two-Stage seismic isolation method; Two-Stage Friction Pendulum Bearing; hysteresis characteristic; seismic isolation; resilience

check for updates

Citation: Peng, T.; Guan, J.; Wu, Y. Numerical and Experimental Investigation of the Seismic Effect of a Two-Stage Seismic Isolation Method. *Sustainability* **2023**, *15*, 4883. https://doi.org/10.3390/su15064883

Academic Editor: Stefano Galassi

Received: 15 December 2022
Revised: 1 February 2023
Accepted: 6 March 2023
Published: 9 March 2023

Copyright: © 2023 by the authors. Licensee MDPI, Basel, Switzerland. This article is an open access article distributed under the terms and conditions of the Creative Commons Attribution (CC BY) license (https://creativecommons.org/licenses/by/4.0/).

1. Introduction

Earthquakes are one of the most devastating disasters faced by structures, and structural collapses are responsible for a high mortality rate during earthquakes. Therefore, to protect structures from earthquakes, many seismic protection methods have been proposed and developed.

The earliest seismic design method is the strength design method. Through the strength design of key components, this method can theoretically protect all components from seismic damage. The disadvantage of this method is that the key components need to be designed rather thick, which may require more materials. In addition, a greater mass may cause a greater inertial force, requiring further enlargement of the section and all the components, thus requiring more materials, resulting in a vicious cycle.

The ductility design method solves the problem of the strength design method to some extent. It divides all the components into ductile components and capacity protection components, and sets the plastic hinge regions in the ductile components. Allowing the plastic hinge regions to experience controllable damage in earthquakes, this method can protect the integrity of all the capacity protection components, so as to avoid the problem that the components are rather thick. However, its disadvantage is that the damage of the plastic hinge regions in earthquakes will affect the normal operation, and the repair after earthquakes also needs a lot of time and cost.

The seismic isolation method developed in recent years inherits the idea of the ductility design method. However, the difficulty of post-earthquake repair can be reduced by

transferring the damage in the plastic hinge regions to the seismic isolation bearings. This is the most effective method to improve the seismic performances of bridge structures. The main idea of seismic isolation is to uncouple a structure from horizontal ground motions to decrease structural acceleration and force responses by seismic isolation bearings, such as friction pendulum bearing (FPB for short), lead rubber bearing and high damping rubber bearing. Among all seismic isolation bearings, the FPB is the most well-known. This kind of bearing was first proposed by Zayas et al. of the University of California, Berkeley, USA in 1985 [1]. A traditional FPB is composed of an upper plate with a concave surface, a lower plate with a concave surface, a slider and two friction pairs, as shown in Figure 1. Several studies have shown that FPBs have many remarkable features, including high vertical bearing capacity, good durability, easy installation and large displacement capacity [2–5]. The main drawback of FPB is the limited energy dissipation capacity under extreme earthquakes [6].

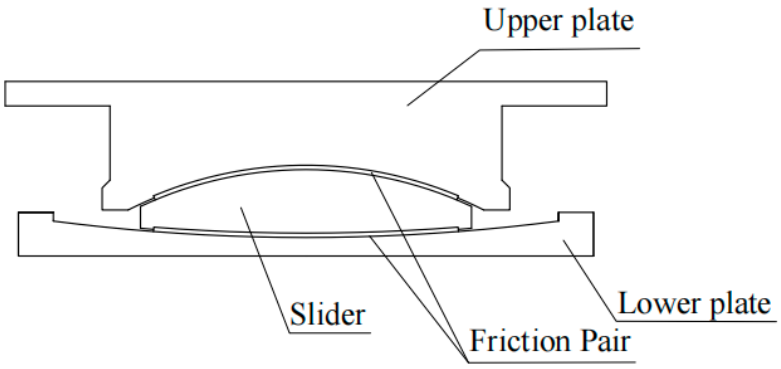


Figure 1. The diagram of a traditional FPB.

In the analysis of the restoring force of FPBs, the dynamic friction coefficient and geometry of the concave surface are the two main factors and have been widely studied and optimized [7–10]. A traditional FPB has a fixed friction coefficient; many researchers have studied the influence of the friction coefficient on the structural seismic performance and proved the existence of the optimal friction coefficient. This optimal parameter is related to the design objective and ground motion characteristics. Jangid studied the stochastic response of bridges seismically isolated by the FPS and the influence of system parameters such as isolation period, frequency content, and intensity of an earthquake on the optimum friction coefficient of FPS. A closed form expression for the optimum friction coefficient of FPS and corresponding response of the isolated bridge system were proposed, and it was proved to have a good comparison between the proposed closed form expressions, actual optimum parameters and the response of the isolated bridge system [11]. Shahbazi et al. used two polynomial functions to express the surface characteristics and the most proper function was explored to minimize the structural accelerations and isolator displacements. It was found that the optimal friction coefficient increases with the increase of seismic intensity and the polynomial function of order six has the least possible structural acceleration [12]. The above studies were concerned with a fixed friction coefficient. In addition, some scholars have proposed a new kind of FPB with a variable friction coefficient on the sliding surface (VFPB for short) [13]. The sliding surface of the bearing was coated with different friction materials, each with different friction coefficients. When the slider slides on the concave surface, the friction coefficient would change with the increase of the displacement [14].

With the in-depth study of FPBs and the accumulation of practical experience, several new kinds of bearings have been developed based on the traditional FPB. Murnal et al. developed a new kind of variable frequency pendulum isolator (VFPI for short) with different curvature radii on the sliding surface to overcome the limitations when the input excitation level is significantly different from its design level [15,16]. The mathematical

formulation for the three-dimensional behavior of VFPI and the torsional performance were derived through mechanical analysis and verified by finite element analysis. It has been shown that isolating a structure using VFPI is very effective for vibration control of structure–equipment and other primary–secondary systems. The radius of the curvature of VCFPS is lengthened with an increase of the isolator displacement, so the basic period of a base-isolated structure can be far away from the main period of near-fault ground motion [17].

Another improvement method is to increase the number of sliders. The method was first proposed by Morgan [18], and behavior of a new kind of Multiple Friction Pendulum System (MFPB for short) was compared with both nonlinear viscous and bilinear hysteretic energy dissipation mechanisms. An MFPB was designed and studied through full-scale component and shaking table tests. These test results demonstrated that the MFPS isolator possessed excellent durability and outstanding earthquake-proof capability [19]. Fenz developed a new kind of Triple-Friction Bearing (TFPB for short) consisting of four sliding surfaces with different curvature radii and friction coefficients [20,21]. Different combinations of curvature radii, displacement capacities and friction coefficients ensured the TFPB has adaptive stiffness, good energy dissipation capacity and large horizontal displacement capacity [22–26].

New kinds of FPBs can also be invented by combining a traditional FPB with other devices or new types of sliders. A new type of frictional device, the Lateral Impact Resilient double concave Friction Pendulum (LIR-DCFP) bearing was invented and the device had an improved inner slider to enhance the dynamic behavior [27]. A new type of shape memory alloy cable double friction pendulum bearing (SCDFPB) composite isolator was invented, which combined the FPB with the super-elastic shape memory alloy (SMA) cable. The hysteresis characteristic of SCDFPBs was studied and the results showed that SCDFPBs had an adaptive capability to multi-level earthquake intensities [28–30]. Pang proposed a hybrid isolation system composed of two FPBs and super-elastic shape memory alloy (SMA) cables. The system can provide additional control force through SMA cables to limit the bearing displacement with synergistic energy dissipation and adapt to different seismic intensities [31].

The Shock transmission unit, also called a Lock-up device, is a common-used bridge seismic device which is similar to a rigid connection to make all the piers of the structure bear the seismic load together [32–34]. Some scholars proposed to install the Lock-up device on the FPB to control the different working modes of the bearing under the normal operation of the bridge and different seismic intensities. The increased acceleration of the girder under a large earthquake will make the Lock-up device lock the movement of all the expansion bearings and turn them into FPBs. In this way, all the piers can jointly bear the seismic force, and the internal force of fixed piers and the displacement of the girder are both reduced.

The seismic isolation method using traditional FPBs cannot restrict effectively maximum displacements and residual displacements simultaneously, and therefore a Two-Stage seismic isolation method is developed in this paper. Based on the method, a new kind of isolation device, Two-Stage Friction Pendulum Bearing (TSFPB for short), was invented to accomplish the goal of the method based on traditional FPBs. In the following sections, the geometry configuration and sliding states of TSFPBs are introduced and the hysteresis characteristics are first investigated experimentally. Then a numerical analysis for an actual highway girder bridge is carried out to analyze the seismic effect. The seismic effects of traditional seismic isolation bearings and TSFPB are thereafter studied and compared. Finally, the seismic isolation mechanism of the suggested seismic isolation method is discussed.

2. Hysteresis Characteristics of TSFPBs

2.1. Geometry of a TSFPB

The most distinguishing feature of a TSFPB different from a traditional FPB is that a TSFPB is composed of four parts: the upper plate, the upper slider with blocks, the lower

slider and the lower plate, as shown in Figure 2. It has three sliding surfaces, each of which has a friction pair. The three sliding surfaces are independent of each other and can have different radii of curvature and friction coefficients. Each physical parameter can be separately designed, and the behavior of a TSFPB is controlled by different combinations of parameters.

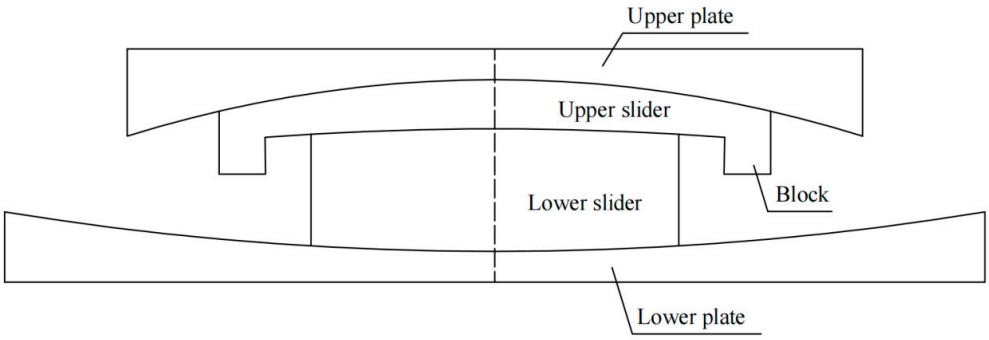


Figure 2. Configuration of a TSFPB.

2.2. Sliding States

A TSFPB has three friction surfaces but only two friction surfaces are designed to slide simultaneously. According to different curvature radii and friction coefficients, two sliding states are arranged: Middle-Lower sliding and Upper-Lower sliding, as shown in Figure 3. The red line is the friction surface used for sliding in two states.



(**a**) (**b**)

Figure 3. Diagram of the two sliding states. (**a**) Middle-Lower sliding state; (**b**) Upper-Lower sliding state.

Middle-Lower sliding state: The upper plate and upper slider move together like one component, and the middle and lower sliding surfaces slide simultaneously. The sliding state and performance of a TSFPB are equivalent to a traditional FPB with a thicker upper plate.

Upper-Lower sliding state: The upper and lower sliders move together like one component, and the upper and lower sliding surfaces slide simultaneously. The sliding state and performance of a TSFPB are equivalent to a traditional FPB with a thicker slider.

Reducing friction coefficients of middle and lower sliding surfaces and increasing that of the upper sliding surface, Middle-Lower sliding would take place first in the event of an earthquake. If the seismic intensity is not very great, the bearing displacement is limited and the lower slider and the blocks of the upper slider will not touch each other. The seismic performance of a TSFPB is equivalent to a traditional FPB with smaller initial sliding friction force, sliding stiffness and horizontal displacement. This is Stage I of the Two-Stage seismic isolation method.

If the seismic intensity becomes greater, the bearing displacement is larger and the gap between the lower slider and the blocks will disappear. If the bearing displacement continues to increase, Upper-Lower sliding would take place then. The Upper-Lower sliding occurs with larger initial sliding friction force, sliding stiffness and horizontal displacement. This is Stage II of the Two-Stage seismic isolation method.

In Stage II, if the bearing displacement decreases from the maximum value, Middle-Lower sliding would take place before Upper-Lower sliding. Therefore, the initial sliding

friction force and sliding stiffness of unloading are less than those of loading, and the residual displacement is thus reduced to improve the post-earthquake resilience of structures.

2.3. Hysteresis Characteristics

Formulas of restoring forces of a TSFPB in each stage can be obtained based on the moment balance theory [9]. For Stage I,

$$F = k_1 d + f_{y1}\mathrm{sgn}\dot{d} \tag{1}$$

$$f_{y1} = \frac{\mu_l R_l W + \mu_m R_m W}{R_l + R_m - h_l} \tag{2}$$

$$k_1 = \frac{W}{R_l + R_m - h_l} \tag{3}$$

For Stage II,

$$F = k_2 d + f_{y2}\mathrm{sgn}\dot{d} \tag{4}$$

$$f_{y2} = \frac{\mu_u R_u W + \mu_l R_l W}{R_u + R_l - h_u - h_l} \tag{5}$$

$$k_2 = \frac{W}{R_u + R_l - h_u - h_l} \tag{6}$$

where, R_u, R_m and R_l are curvature radii of upper, middle and lower sliding surfaces; μ_u μ_m and μ_l are friction coefficients of upper, middle and lower sliding surfaces; h_u is the minimum thickness of the upper slider; h_l is the maximum thickness of the lower slider; d_{th} is the horizontal distance between the block and the lower slider; d is the horizontal displacement of the bearing; W is the vertical load of the bearing; k_1 and k_2 are sliding stiffnesses in Stage I and II, respectively; and f_{y1} and f_{y2} are initial sliding friction forces in Stage I and II, respectively.

Parameters of these Equations are illustrated in Figure 4.

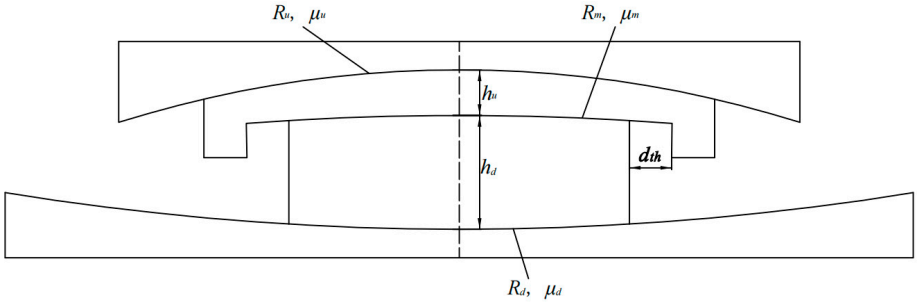


Figure 4. Description of parameters.

The relation between restoring force and horizontal displacement is shown in Figure 5.

In order to verify the correctness of the hysteresis curve of the TSFPB, the specimen of the bearing was designed and fabricated, and a quasi-static test was carried out. The specimen before the test is shown in Figure 6. Main parameters of the specimen are listed in Table 1. Among them, friction coefficients of sliding surfaces are calculated according to the results of a friction test.

The quasi-static test was conducted in the State Key Laboratory of Disaster Reduction in Civil Engineering of Tongji University. The testing device and the specimen in the test are presented in Figures 7 and 8.

The influence of the vertical load on FPBs is significant. It is found that the horizontal stiffness of the FPB increases with the increase of the vertical load, the area of the hysteresis loop increases, and the energy dissipation capacity also increases [35–37]. As a kind of FPBs, these rules can be also applied to TSFPBs.

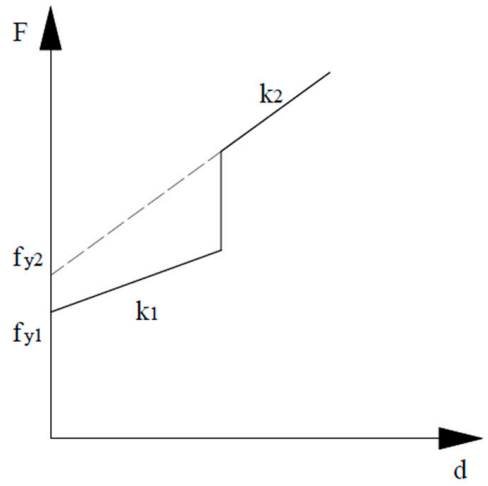


Figure 5. The relation between restoring force and horizontal displacement.



Figure 6. The specimen before the test.

Table 1. Main parameters of the specimen.

Parameters	Value	Parameters	Value
R_u	500 mm	μ_u	0.0664
R_m	1500 mm	μ_m	0.0264
R_l	2000 mm	μ_l	0.0264
h_u	35 mm	h_d	75 mm

During the test, the vertical load was kept as 1000 kN. The horizontal load was applied cyclically by the displacement control mode, and the displacement amplitudes were 150 mm and 180 mm.

According to the test results, the relationship between restoring force F_h and horizontal displacement d was plotted and compared with the hysteresis curve of the theoretical analysis, as shown in Figure 9.

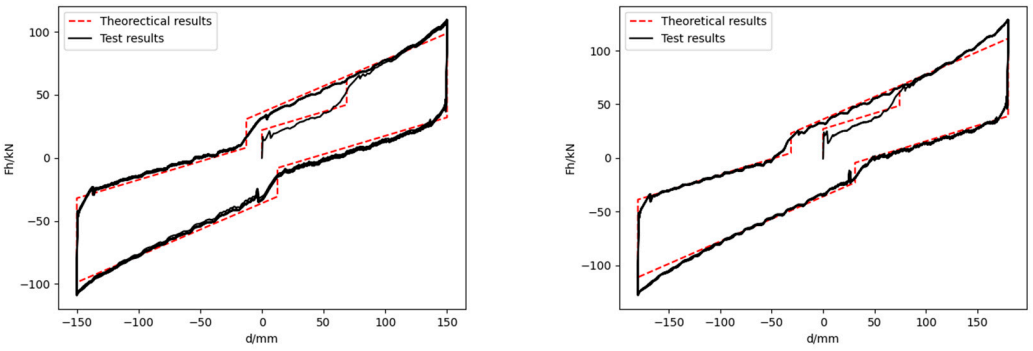
As shown, the test results are in good agreement with the theoretical results, especially in the range of small displacements. However, there is some deviation of horizontal force in the range of large displacements, which is mainly because the theoretical analysis assumes that the bearing displacement is much smaller than the curvature radius of each sliding surface of the bearing. This assumption is true in the range of small displacements, but there will be some errors in the range of large displacements.



Figure 7. The test device.



Figure 8. The specimen in the test.



(**a**) (**b**)

Figure 9. Comparison of hysteresis curves of the test and theoretical results. (**a**) Hysteresis curve of d_{max} = 150 mm; (**b**) Hysteresis curve of d_{max} = 180 mm.

2.4. Simulation Method of the TSFPB

According to the hysteresis characteristics, the finite element simulation method of the TSFPB is studied in this section.

For bearings with blocks, hook element and gap element are usually used to simulate the resistance of blocks [38–40]. Therefore, they are also used in the TSFPB model. The TSFPB model can be constructed by four basic elements in series and parallel. An element Bouc-Wen 1 is connected in parallel with a hook element and a gap element, and then the three elements are connected in series with an element Bouc-Wen 2. The simulation method is illustrated in Figure 10.

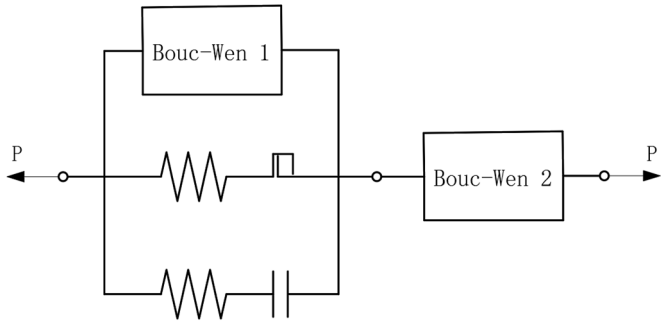


Figure 10. The simulation method of a TSFPB.

Among them, the element Bouc-Wen 1 is used to simulate the Middle-Lower sliding of the TSFPB. The parameters of Bouc-Wen 1 are set according to the Middle-Lower sliding state of the bearing. The hook element and gap element are used to simulate the contact between the block and the lower slider. The element Bouc-Wen 2 is used to simulate the Upper-Lower sliding state. The parameters of Bouc-Wen 2 are set according to the Upper-Lower sliding state of the bearing.

Calculation methods of all the element parameters are listed in Table 2.

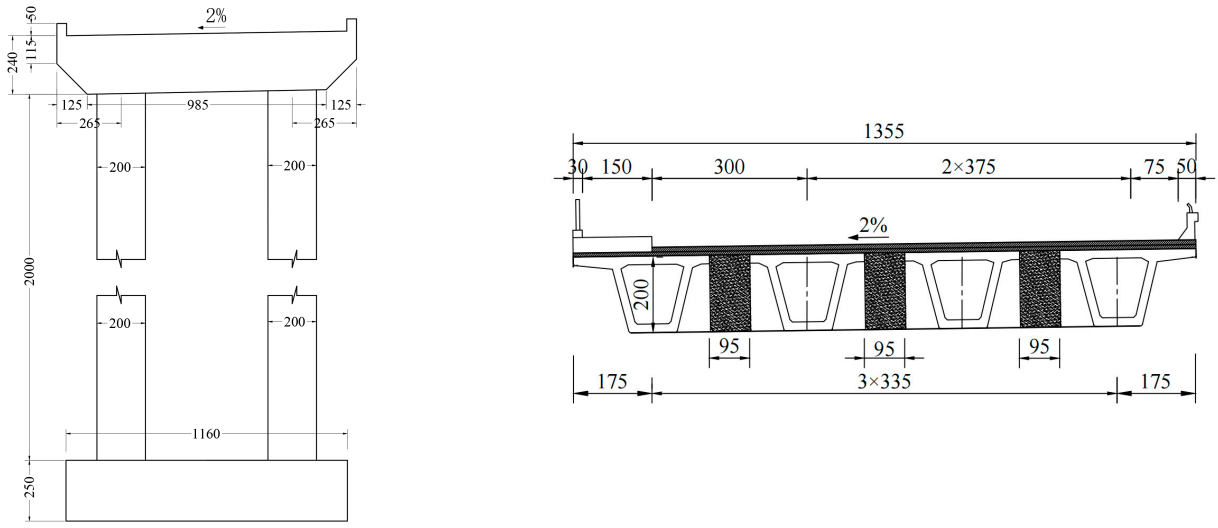
Table 2. Calculation methods of all the element parameters.

Elements	Parameters	Calculation Method
Bouc-Wen 1	initial stiffness initial sliding friction force f_{y1} sliding stiffness k_1	Take a large number, such as 10^6 kN/m Calculate via Equation (2) Calculate via Equation (3)
Hook	initial stiffness open	Take a large number, such as 10^6 kN/m Equals d_{th}
Gap	initial stiffness open	Take a large number, such as 10^6 kN/m Equals d_{th}
Bouc-Wen 2	initial stiffness initial sliding friction force f_{y2} sliding stiffness k_2	Take a large number, such as 10^6 kN/m Calculate via Equation (5) Calculate via Equation (6)

3. Seismic Effect of the Two-Stage Seismic Isolation Method

3.1. The Bridge Example

In order to compare the seismic design method recommended in this paper with the seismic isolation method using traditional FPBs, and to investigate its seismic effect, a simply-supported girder bridge with a span of 35 m is used as an example, as shown in Figure 11. The girder is composed of four small box girders. The pier is composed of a cap beam and two columns fixed on a pile cap. All the piers are fixed on the ground. Details of the bridge are listed in Table 3. The finite element model is established in SAP2000, and uses the non-linear modal superposition FNA method.



(a) (unit:cm) (b) (unti:cm)

Figure 11. Structural dimensions of the bridge. (**a**) Elevation of the pier; (**b**) Cross section of the girder.

Table 3. Details of the bridge.

Components	Material	Cross Section (m)	Length (m)
Girder	C50 reinforced concrete	Four small box girders	35
Cap beam	C40 reinforced concrete	A rectangle of 2.2 × 2.4	12.35
Column	C40 reinforced concrete	A circle with a diameter of 2.0	20
Pile cap	C40 reinforced concrete	A rectangle of 6 × 2.5	11.6

3.2. Seismic Input

According to Specifications for Seismic Design of Highway Bridges (JTG/T 2231-01-2020) [41], the bridge category is Class B. The acceleration peak of the basic ground motion is 0.2 g, and the site category is Class III. In this analysis, two levels of ground motion input were used, and the return periods of Level I and II are 75 and 2000 years respectively. Six artificial ground motions were generated and shown in Figure 12. Among them, Wave 1, 2 and 3 correspond to seismic intensity Level I, and Wave 4, 5 and 6 correspond to seismic intensity Level II. The ground motions are inputted along the transverse direction of the bridge.

3.3. Analysis Models

A total of three different analysis models were built to compare the recommended seismic design method with the seismic isolation method using traditional FPBs. The three models have the same bridge structure and different bearings. In the first two models, traditional FPBs are used. The difference between the first two models is that bearings in the first model (FPB1 for short) have a smaller initial sliding friction force and bearings in the second model (FPB2 for short) have a larger initial sliding friction force. In the third model, TSFPBs are used.

Hysteresis parameters of all the three bearings are listed in Table 4. Hysteresis curves of all the three bearings are shown in Figure 13.

3.4. Seismic Responses

Time-histories of the bearing displacements and the bending moments at the column bottom under ground motion Wave 1 are shown in Figure 14, and those under ground

motion Wave 5 are shown in Figure 14. Hysteresis curves of the three bearings under the ground motion Wave 5 are shown in Figure 15.

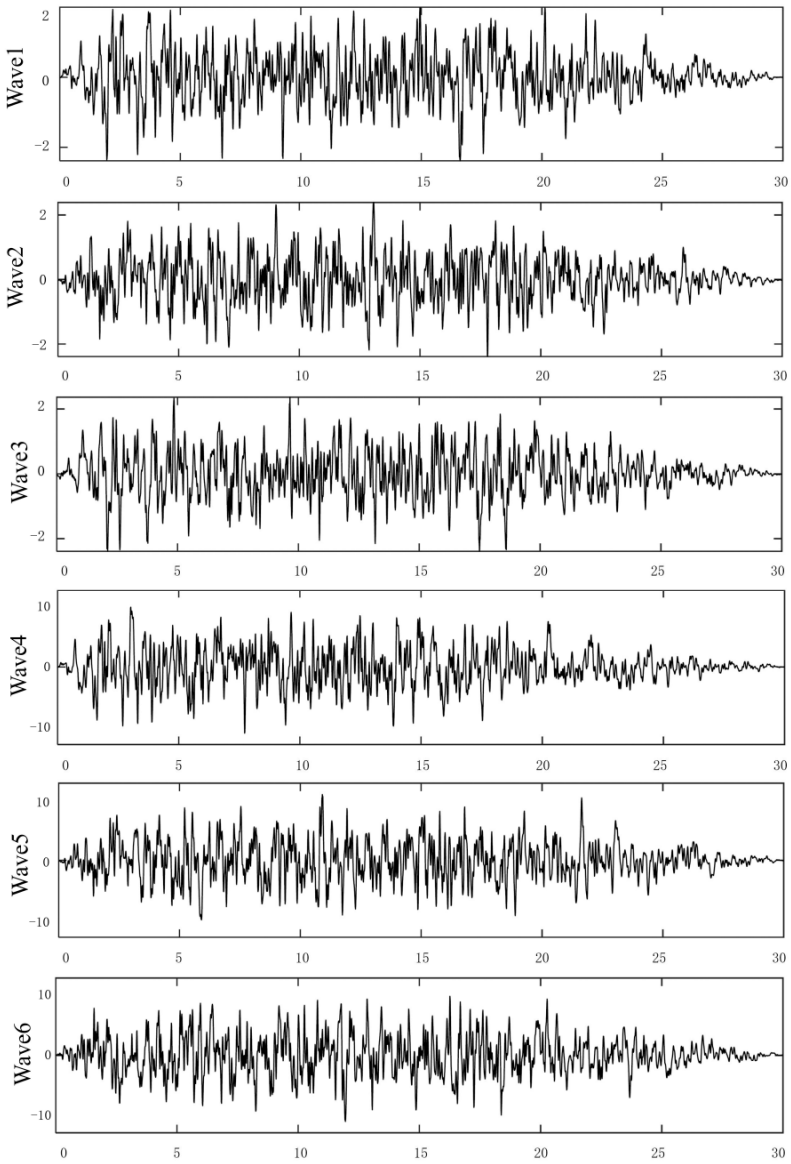


Figure 12. Artificial ground motions (Unit: m/s^2).

Table 4. Hysteresis parameters of bearings.

Models	Bearings	Parameters	Values
Model 1	FPB1	sliding stiffness k	1333 kN/m
		initial sliding friction force f_y	100 kN
Model 2	FPB2	sliding stiffness k	1860 kN/m
		initial sliding friction force f_y	500 kN
Model 3	TSFPB	sliding stiffness k_1	1333 kN/m
		initial sliding friction force f_{y1}	95 kN
		sliding stiffness k_2	1860 kN/m
		initial sliding friction force f_{y2}	500 kN

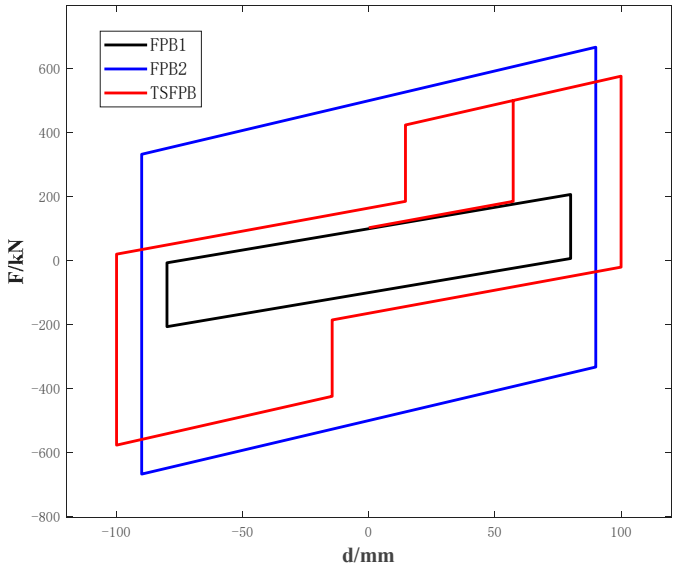
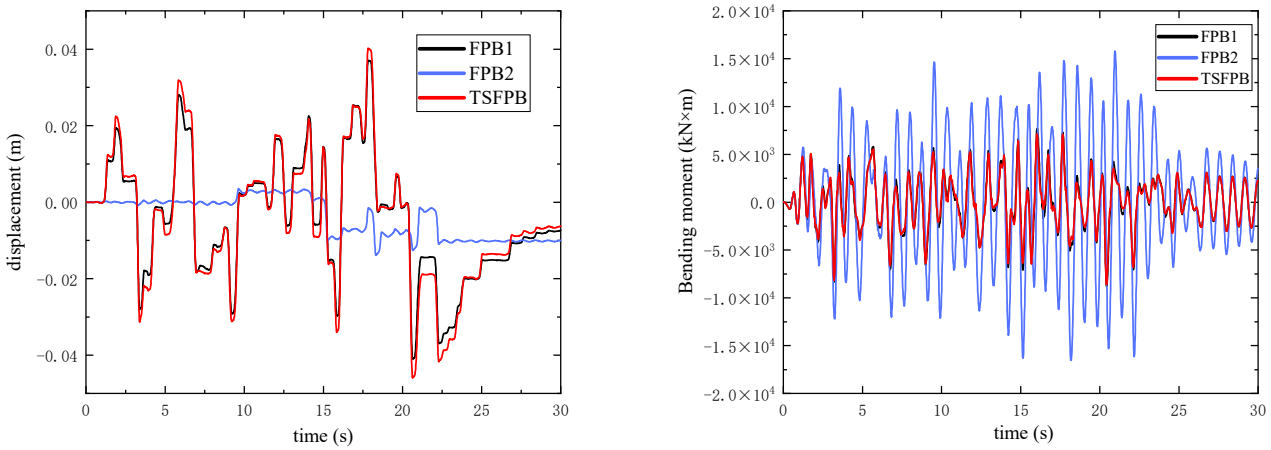


Figure 13. Hysteresis curves of bearings.



(**a**) (**b**)

Figure 14. Two seismic responses under the ground motion Wave 1. (**a**) Bearing displacement; (**b**) Bending moment at the column bottom.

Maximum values of some important seismic responses under all six ground motions are listed in Table 5, including shear forces and bending moments at the column bottom and bearing displacements.

As shown in Figure 14 and Table 5, for the seismic intensity Level I, seismic responses of Model 1 and 3 are almost the same because the TSFPB used in Model 3 is in Stage I and the hysteresis parameters of the TSFPB in Stage I are very close to those of FPB1 used in Model 1. Furthermore, because the sliding stiffness and initial sliding friction force of FPB1 are both much smaller than those of FPB2, bearing displacements of Model 1 and 3 are both larger than those of Model 2, and shear forces and bending moments at the column bottom of Model 1 and 3 are both much smaller than those of Model 2.

As shown from Figures 14 and 15 and Table 5, for the seismic intensity Level II, seismic responses of Model 3 are very desirable. On the one hand, shear forces and bending moments at the column bottom of Model 3 are much smaller than those of Model 2 and not much larger than those of Model 1. On the other hand, bearing displacements of Model 3 are the least, and only about half of those of Model 1.

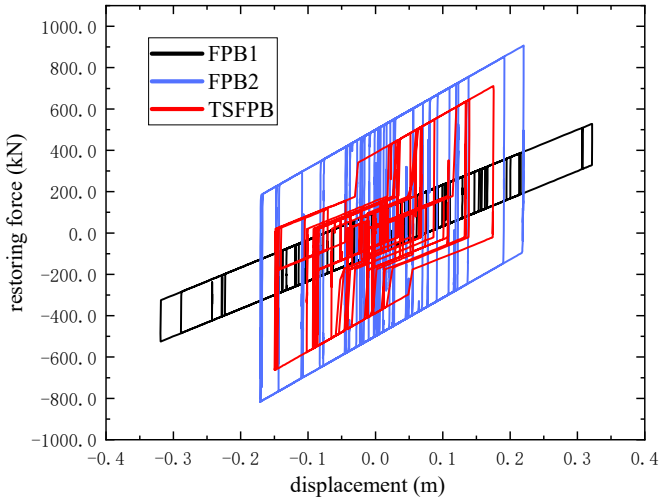


Figure 15. Hysteresis curves of the three bearings under the ground motion Wave 5.

Table 5. Some seismic responses under all the six ground motions.

Seismic Intensity	Case	Model	Shear Force at the Column Bottom (kN)	Bending Moment at the Column Bottom (kN/m)	Bearing Displacement (m)
Level I	Wave 1	Model 1	891	8791	0.0410
		Model 2	1669	16,544	0.0139
		Model 3	876	8606	0.0460
	Wave 2	Model 1	904	9081	0.0429
		Model 2	1782	17,662	0.0162
		Model 3	898	8948	0.0507
	Wave 3	Model 1	749	7405	0.0350
		Model 2	1716	17,177	0.0177
		Model 3	713	7050	0.0396
Level II	Wave 4	Model 1	2707	26,609	0.2568
		Model 2	3436	33,923	0.1957
		Model 3	2644	25,709	0.1596
	Wave 5	Model 1	2751	27,676	0.3219
		Model 2	3451	34,010	0.2202
		Model 3	2541	24,981	0.1755
	Wave 6	Model 1	2511	24,301	0.3140
		Model 2	3267	31,276	0.2103
		Model 3	2629	25,622	0.1616

In summary, the Two-Stage seismic isolation method has been proven to be adaptable to different seismic intensities. When the seismic intensity level is low, the method does not limit the relative displacement between piers and the girder. The TSFPBs used in this method work in Stage I like FPBs with a smaller sliding stiffness and initial sliding friction force. The bridge superstructure is isolated from ground motions. Therefore, the internal forces of the bridge structure are reduced, and the structure remains elastic and undamaged in minor earthquakes.

When the seismic intensity level is high, the TSFPBs used in this method work in Stage II like FPBs with a larger sliding stiffness and initial sliding friction force. More energy is dissipated by the larger sliding stiffness and friction force, and therefore the bearing displacement is reduced. Then the bridge structure is protected from structural damage and unseating of the superstructure.

When the earthquake comes to an end, the TSFPBs used in this method returns to Stage I and the residual displacement of the bridge is smaller due to the smaller friction force. Therefore, TSFPBs show better post-earthquake resilience than traditional FPBs.

4. Conclusions

In this paper, a Two-Stage seismic isolation method is proposed to effectively restrict maximum displacements and residual displacements simultaneously. Therefore, a new kind of seismic isolation bearing, Two-Stage Friction Pendulum Bearing, was developed and introduced. Its hysteresis curve was verified experimentally and the simulation method of the bearing in an FEM software was proposed. A numerical analysis for an actual highway girder bridge was carried out to compare the seismic design method recommended in this paper with the conventional seismic isolation method. The main conclusions are as follows:

1. The Two-Stage seismic isolation method has adaptive restoring force, horizontal stiffness and energy dissipation mechanism for different seismic intensity levels, and better seismic performance compared with conventional seismic isolation method.
2. Bridges with TSFPBs have smaller residual displacements and better post-earthquake resilience than those with traditional FPBs.

Author Contributions: Conceptualization, T.P.; Writing—original draft, J.G.; Writing—review & editing, T.P.; Supervision, T.P. and Y.W. All authors have read and agreed to the published version of the manuscript.

Funding: This work was supported by the Ministry of Science and Technology of China (Grant No. SLDRCE19-B-21), and the National Natural Science Foundation of China (Grant No. 51278372 and No. 51878489).

Data Availability Statement: Some or all data, models, or codes that support the findings of this study are available from the corresponding author upon reasonable request.

Conflicts of Interest: The authors declare that they have no known competing financial interest or personal relationship that could have appeared to influence the work reported in this paper.

References

1. Zayas, V.A.; Low, S.S.; Mahin, S.A. *FPS (Friction Pendulum System) Earthquake Resisting System. Experimental Report*; California Univ., Richmond. Earthquake Engineering Research Center, Earthquake Protection Systems: San Francisco, CA, USA, 1987.
2. Calvi, P.M.; Calvi, G.M. Historical Development of Friction-Based Seismic Isolation Systems. *Soil Dyn. Earthq. Eng.* **2018**, *106*, 14–30. [CrossRef]
3. Landi, L.; Grazi, G.; Diotallevi, P.P. Comparison of Different Models for Friction Pendulum Isolators in Structures Subjected to Horizontal and Vertical Ground Motions. *Soil Dyn. Earthq. Eng.* **2016**, *81*, 75–83. [CrossRef]
4. Braun, C. The Sliding Isolation Pendulum—An Improved Recentring Bridge Bearing. *Steel Constr.* **2009**, *2*, 203–206. [CrossRef]
5. Zhuang, P.; Wei, L.; Han, M. Seismic Performance Assessment of a Single-Layer Spherical Lattice Shell Structure with Multifunctional Friction Pendulum Bearings. *Int. J. Struct. Stab. Dyn.* **2022**, *22*, 2250119. [CrossRef]
6. Ismail, M.; Rodellar, J.; Ikhouane, F. An Innovative Isolation Device for Aseismic Design. *Eng. Struct.* **2010**, *32*, 1168–1183. [CrossRef]
7. Lin, B.-C.; Tadjbakhsh, I.; Papageorgiou, A.; Ahmadi, G. Performance of Earthquake Isolation Systems. *J. Eng. Mech. ASCE* **1990**, *116*, 446–461. [CrossRef]
8. Peng, T.; Yan, B.; Li, F. The Hysteresis Model of the Friction Pendulum Bearing Based on the Moment Balance Theory. *Ain Shams Eng. J.* **2022**, *13*, 101707. [CrossRef]
9. Mokha, A.; Constantinou, M.; Reinhorn, A. Teflon Bearings in Base Isolation I: Testing. *J. Struct. Eng.* **1990**, *116*, 438–454. [CrossRef]
10. Vibhute, A.S.; Bharati, S.D.; Shrimali, M.K.; Datta, T.K. Optimum Coefficient of Friction in FPS for Base Isolation of Building Frames. *Pract. Period. Struct. Des. Constr.* **2022**, *27*, 04022042. [CrossRef]
11. Jangid, R. Stochastic Response of Bridges Seismically Isolated by Friction Pendulum System. *J. Bridge Eng.* **2008**, *13*, 319–330. [CrossRef]
12. Shahbazi, P.; Taghikhany, T. Sensitivity Analysis of Variable Curvature Friction Pendulum Isolator under Near-Fault Ground Motions. *Smart Struct. Syst.* **2017**, *20*, 23–33.
13. Downey, A.; Theisen, C.; Murphy, H.; Anastasi, N.; Laflamme, S. Cam-Based Passive Variable Friction Device for Structural Control. *Eng. Struct.* **2019**, *188*, 430–439. [CrossRef]

14. Timsina, S.; Calvi, P. Variable Friction Base Isolation Systems: Seismic Performance and Preliminary Design. *J. Earthq. Eng.* **2018**, *25*, 1–24. [CrossRef]
15. Murnal, P.; Sinha, R. Aseismic Design of Structure–Equipment Systems Using Variable Frequency Pendulum Isolator. *Nucl. Eng. Des.* **2004**, *231*, 129–139. [CrossRef]
16. Murnal, P.; Sinha, R. Behavior of Torsionally Coupled Structures with Variable Frequency Pendulum Isolator. *J. Struct. Eng. -ASCE* **2004**, *130*, 1041–1054. [CrossRef]
17. Tsai, C.S.; Chiang, T.-C.; Chen, B.-J. Finite Element Formulations and Theoretical Study for Variable Curvature Friction Pendulum System. *Eng. Struct.* **2003**, *25*, 1719–1730. [CrossRef]
18. Morgan, T.A. The Use of Innovative Base Isolation Systems to Achieve Complex Seismic Performance Objectives. Ph.D. Thesis, University of California, Berkeley, CA, USA.
19. Tsai, C.; Chen, W.-S.; Chiang, T.-C.; Chen, B.-J. Component and Shaking Table Tests for Full-Scale Multiple Friction Pendulum System. *Earthq. Eng. Struct. Dyn.* **2006**, *35*, 1653–1675. [CrossRef]
20. Fenz, D.M.; Constantinou, M.C. Spherical Sliding Isolation Bearings with Adaptive Behavior: Theory. *Earthq. Eng. Struct. Dyn.* **2008**, *37*, 163–183. [CrossRef]
21. Fenz, D.M.; Constantinou, M.C. Spherical Sliding Isolation Bearings with Adaptive Behavior: Experimental Verification. *Earthq. Eng. Struct. Dyn.* **2008**, *37*, 185–205. [CrossRef]
22. Shang, J.; Tan, P.; Zhang, Y.; Han, J.; Mi, P. Seismic Isolation Design of Structure Using Variable Friction Pendulum Bearings. *Soil Dyn. Earthq. Eng.* **2021**, *148*, 106855. [CrossRef]
23. Loghman, V.; Khoshnoudian, F.; Banazadeh, M. Effect of Vertical Component of Earthquake on Seismic Responses of Triple Concave Friction Pendulum Base-Isolated Structures. *J. Vib. Control* **2015**, *21*, 2099–2113. [CrossRef]
24. Dhankot, M.; Soni, D. Behaviour of Triple Friction Pendulum Isolator under Forward Directivity and Fling Step Effect. *KSCE J. Civ. Eng.* **2016**, *21*, 872–881. [CrossRef]
25. Tajammolian, H.; Khoshnoudian, F. Acceleration Amplification Due to Rotational Components of Near-Fault Earthquakes in Triple Concave Friction Pendulum Base-Isolated Structures. *Can. J. Civ. Eng.* **2018**, *45*, 314–327. [CrossRef]
26. Xu, Y.; Becker, T.C.; Guo, T. Design Optimization of Triple Friction Pendulums for High-Rise Buildings Considering Both Seismic and Wind Loads. *Soil Dyn. Earthq. Eng.* **2021**, *142*, 106568. [CrossRef]
27. Auad, G.; Almazán, J.L. Lateral Impact Resilient Double Concave Friction Pendulum (LIR-DCFP) Bearing: Formulation, Parametric Study of the Slider and Three-Dimensional Numerical Example. *Eng. Struct.* **2021**, *233*, 111892. [CrossRef]
28. Peng, Z.; Wei, W.; Yibo, L.; Miao, H. Cyclic Behavior of an Adaptive Seismic Isolation System Combining a Double Friction Pendulum Bearing and Shape Memory Alloy Cables. *Smart Mater. Struct.* **2021**, *30*, 075003. [CrossRef]
29. Zheng, W.; Wang, H.; Li, J.; Huijun, S. Parametric Study of SMA-Based Friction Pendulum System for Response Control of Bridges under Near-Fault Ground Motions. *J. Earthq. Eng.* **2021**, *25*, 1494–1512. [CrossRef]
30. Zheng, W.; Wang, H.; Li, J.; Shen, H. Performance Evaluation of Bridges Isolated with SMA-Based Friction Pendulum System at Low Temperatures. *Soil Dyn. Earthq. Eng.* **2019**, *125*, 105734. [CrossRef]
31. Pang, Y.; He, W.; Zhong, J. Risk-Based Design and Optimization of Shape Memory Alloy Restrained Sliding Bearings for Highway Bridges under near-Fault Ground Motions. *Eng. Struct.* **2021**, *241*, 112421. [CrossRef]
32. Zhang, Y.-L.; Dong, Y.; Zhu, S.-Q.; Chen, X.-C.; Ding, M.-B. Research on the Damping Performance of the Long-Span Deck Type Steel Truss Railway Arch Bridge. *J. Railw. Eng. Soc.* **2016**, *33*, 75–79.
33. Wang, Y.; Dai, G. Seismic Response and Cushioning Research of Long-Span Railway Continuous Beam-Arch Composite Bridge. *IABSE Symp. Rep.* **2015**, *105*, 1–5.
34. Li, X.-B. Research on the Mechanism of Longitudinal Seismic Mitigation Devices for High-Speed Railway Continuous Bridges. *J. Railw. Eng. Soc.* **2017**, *34*, 50–56.
35. Hoang, P.H.; Phan, H.N.; Nguyen, V.N. On the Influence of the Vertical Earthquake Component on Structural Responses of High-Rise Buildings Isolated with Double Friction Pendulum Bearings. *Appl. Sci.* **2021**, *11*, 3809. [CrossRef]
36. Raftoyiannis, I.G.; Michaltsos, G.T. The Influence of the Vertical Inertia Forces on the Behavior of Friction Pendulum Bearings (FPB). *Arch. Appl. Mech.* **2017**, *87*, 427–437. [CrossRef]
37. Shang, J.; Tan, P.; Zhang, Y.; Han, J.; Qin, J. Experimental and Analytical Investigation of Variable Friction Pendulum Isolator. *Eng. Struct.* **2021**, *243*, 112575. [CrossRef]
38. Nguyen, N.V.; Hoang, H.P.; Huong, K.T. Performance of Single Friction Pendulum Bearing for Isolated Buildings Subjected to Seismic Actions in Vietnam. *IOP Conf. Ser. Earth Environ. Sci.* **2018**, *143*, 012048. [CrossRef]
39. Fenz, D.; Constantinou, M. Modeling Triple Friction Pendulum Bearings for Response-History Analysis. *Earthq. Spectra* **2008**, *24*, 1011–1028. [CrossRef]
40. Bianco, V.; Bernardini, D.; Mollaioli, F.; Monti, G. Modeling of the Temperature Rises in Multiple Friction Pendulum Bearings by Means of Thermomechanical Rheological Elements. *Arch. Civ. Mech. Eng.* **2019**, *19*, 171–185. [CrossRef]
41. *JTG/T 2231-01-2020*; Specifications for Seismic Design of Highway Bridges. China Communications Press: Beijing, China, 2020.

Disclaimer/Publisher's Note: The statements, opinions and data contained in all publications are solely those of the individual author(s) and contributor(s) and not of MDPI and/or the editor(s). MDPI and/or the editor(s) disclaim responsibility for any injury to people or property resulting from any ideas, methods, instructions or products referred to in the content.